ELSEVIER

Earth and Planetary Science Letters 160 (1998) 241–255

EPSL

Helium isotope composition of the early Iceland mantle plume inferred from the Tertiary picrites of West Greenland

D.W. Graham [a,*], L.M. Larsen [b,c], B.B. Hanan [d], M. Storey [b], A.K. Pedersen [b,e], J.E. Lupton [f]

[a] College of Oceanic and Atmospheric Sciences, Oregon State University, Corvallis, OR 97331, USA
[b] Danish Lithosphere Center (DLC), Øster Voldgade 10, DK-1350 Copenhagen K, Denmark
[c] Geological Survey of Denmark and Greenland, Thoravej 8, DK-2400 Copenhagen NV, Denmark
[d] Department of Geological Sciences, San Diego State University, San Diego, CA 92182, USA
[e] Geological Museum, Øster Voldgade 5–7, DK-1350 Copenhagen K, Denmark
[f] NOAA, Pacific Marine Environmental Laboratory, Hatfield Marine Science Center, Newport, OR 97365, USA

Received 10 July 1997; accepted 3 May 1998

Abstract

Picrites from the 61 million year old Vaigat Formation of the Nuussuaq Peninsula in West Greenland have $^3He/^4He$ ratios trapped in olivine phenocrysts which range up to 30 times the atmospheric ratio. These high values, measured during gas extraction by crushing in vacuum, are similar to the highest magmatic $^3He/^4He$ ratios found in young terrestrial volcanic rocks. By analogy with young basalts, in which crushing selectively extracts magmatic helium, any significant cosmogenic ^3He appears to be absent in these picrites. Additional evidence for the absence of cosmogenic helium is provided by fusion results on the crushed olivine powders and by a single stepwise crushing experiment, in which only magmatic and radiogenic helium components are resolvable. The West Greenland picrites have Pb, Nd and Sr isotope compositions which overlap those found in picrites from Iceland and in basalts from Loihi Seamount, localities which today also have high $^3He/^4He$ ratios. Isotopic variations in He, Pb, Nd and Sr for the West Greenland picrites are interpreted to largely result from interaction of the early Iceland mantle plume with the upper mantle during plume ascent and dispersion beneath the continental lithosphere. The presence of high $^3He/^4He$ ratios in West Greenland, and the onset of magmatism across the North Atlantic Volcanic Province near 62 Ma, supports the hypothesis for very rapid dispersion (>1 m/year) of mantle plume head material during the earliest stages of plume impact, as predicted in recent numerical simulations of plume behavior during thermal mantle convection with non-Newtonian rheology.

Keywords: helium; isotopes; Greenland; mantle plumes; picrite

1. Introduction

Helium isotopic studies of volcanic rocks have provided important constraints on the style of mantle convection and limits on vertical mass transport from the deeper mantle [1–4]. Magmas derived from the convecting upper mantle, such as mid-ocean ridge basalts (MORB), have $^3He/^4He$ ratios of 7–9 R_A (where R_A is the atmospheric ratio of 1.39×10^{-6}). Many hotspots, such as Hawaii, Iceland, Samoa, Galápagos, Réunion, Yellowstone and the Ethiopian Rift have higher $^3He/^4He$ ratios, ranging to values

* Corresponding author. E-mail: dgraham@oce.orst.edu

0012-821X/98/$19.00
PII S0012-821X(98)00083-1

near 30 R_A, supporting the hypothesis of mantle plumes rising from source regions deep in the Earth. These deep regions must have remained more isolated over geological time than the shallower mantle, and are thereby less degassed of their primordial volatile inventory.

The number of reliable estimates of the initial $^3He/^4He$ ratio in ancient rocks is currently limited [5–9], and is an important restriction to a full understanding of the He isotope evolution of the Earth's mantle. Marty et al. [7] recently showed that high magmatic ratios could be found in flood basalts when they measured $^3He/^4He$ ratios up to 18 R_A in Oligocene lavas from the Ethiopian Rift. The most intriguing result to date is the discovery of very high $^3He/^4He$, up to 39 R_A, in olivine from the 2.7 Ga komatiites of Alexo, Ontario [8]. Other komatiites, however, have ratios well below the atmospheric ratio due to addition of radiogenic helium, and the reason for preservation of the high $^3He/^4He$ at Alexo compared to other localities is not well understood. Several factors can make it difficult to unambiguously determine the initial $^3He/^4He$ of old rocks, including sample alteration, low He contents due to diffusive gas loss, radiogenic production of ^4He, cosmogenic or nucleogenic production of ^3He, and whether helium-retentive minerals such as olivine or clinopyroxene are present. Consequently, studies of helium isotope variations during the early history of a mantle plume's activity, such as during flood basalt volcanism associated with continental breakup, are still in their infancy, as well-preserved and geologically well-constrained lavas much older than 10 Ma need to be studied.

In the North Atlantic, flood basalt magmatism began about 62 million years ago [10–12]. Large outpourings of basalt occurred nearly simultaneously in the Scottish Tertiary Volcanic Province, in northern Ireland, in the Faeroe Islands, in southeast and West Greenland and along the margin of Baffin Island, over a lateral distance of about 2000 km (e.g. [13]). The synchroneity of this volcanism can be explained by partial melting of anomalously hot material derived from a mantle plume head [13,14]. The pattern of volcanism was partly controlled by the location of pre-existing thin spots in the continental lithosphere [15]. Notably, hot Mg-rich magmas were erupted in many of these localities. In this study we report new He and Pb–Nd–Sr isotope results for the extremely fresh picrites of the Vaigat Formation in West Greenland (Fig. 1). These picrites are geochemically similar in many respects to the most enriched picrites found in Iceland today [16,17]. The He and Pb–Nd–Sr isotope results provide strong, additional evidence for the presence of Iceland plume material beneath West Greenland at 61 Ma.

1.1. Background

The earliest Tertiary volcanic rocks in West Greenland are the picrites and Mg-rich basalts of the Vaigat Formation [17–22]. The Vaigat Formation is unusual in that picrites comprise a large proportion of the eruptive units. On Disko Island and the Nuussuaq Peninsula (Fig. 1) the Vaigat Formation covers an area of $\sim$6000 km^2 with an average thickness of $\sim$1 km. The lavas form subaerial flows and subaqueous breccias [20,22,23]. The oldest parts of the succession are present in fault blocks in western Nuussuaq. The stratigraphy is often complicated by rapid lateral facies changes, in which a succession of subaerial lavas may change into a sequence of pillow lavas and hyaloclastite breccias several hundred meters thick, which may then laterally disappear altogether. A number of marker sequences of crustally contaminated basalts, recognizable in the field by their distinct brownish color, have been used to carry through the stratigraphy. The five samples analyzed in this study are from the Nuussuaq Peninsula, and can be stratigraphically arranged from oldest to youngest in the following order (Fig. 1, right panel): 400457 (middle of Anaanaa Member); 362275 (lower Naujánguit Member); 362149 (middle Naujánguit Member); 332788 (lowermost Ordlingassoq Member); 332828 (upper Ordlingassoq Member). Samples and their locations are described in the **EPSL Online Background Dataset** [1] section.

High precision $^{40}Ar/^{39}Ar$ age determinations for three samples of the Vaigat Formation are indistinguishable from each other at the 1σ confidence level [11], with a weighted mean isochron age of 60.7 ± 0.4 Ma. The dated lavas belong to the earliest part of a long, reversely magnetized interval, ap-

[1] http://www.elsevier.nl/locate/epsl,
mirror site: http://www.elsevier.com/locate/epsl

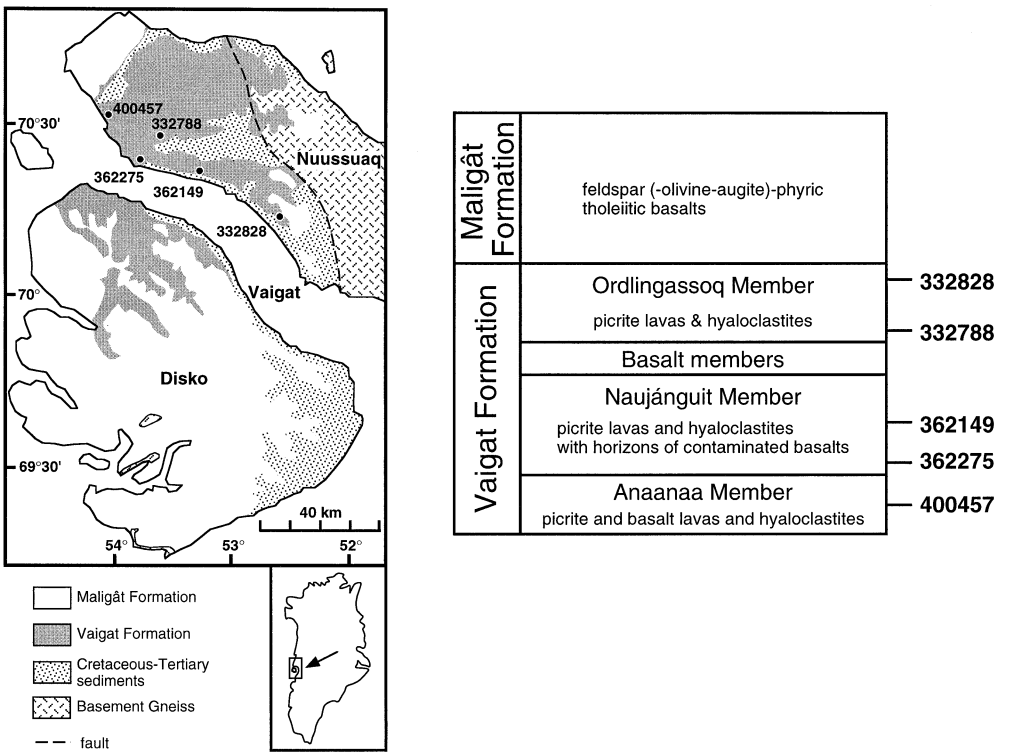

Fig. 1. Location map with GGU sample numbers, and stratigraphic positions of West Greenland picrites from the Nuussuaq Peninsula analyzed for $^{3}He/^{4}He$.

parently Chron 26r (57.9–60.9 Ma). Normally magnetized lavas that must belong to Chron 27n occur low in the Vaigat Formation (60.9–61.3 Ma; [24]), and the two stratigraphically lowest samples in the present work are from this interval. The short duration of Paleocene eruptive activity clearly identifies the sequence as one of rapidly erupted flood lavas [11], with the samples of our study spanning an age range of less than 1 million years.

The picrites of the Vaigat Formation are nearly all tholeiitic in composition, and have been studied earlier in some detail for major and trace elements and Sr, Nd and Pb isotopes [17,21,25]. Those of the Ordlingassoq Member resemble the most enriched picrites from Iceland [17]. The inferred parental magmas have MgO > 19 wt% and SiO_2 near 46 wt%, indicating an origin from hot mantle (potential temperature of 1540°–1600°C) by high degrees of melting (~25%) at moderately high pressure (60 to 90 km depth) [18,26]. Sr and Nd isotope compositions for picrites of the Ordlingassoq Member ($^{87}Sr/^{86}Sr$ = 0.7031–0.7034, ε_{Nd} = 7.5–9.0 at 60 Ma) are enriched relative to North Atlantic MORB, although there is overlap between the two groups. The slightly earlier picrites of the Naujánguit Member range to slightly more depleted isotope compositions (ε_{Nd} up to 10.0). Some of the Naujánguit picrites also show significantly lower ε_{Nd} (down to −3.5), higher $^{87}Sr/^{86}Sr$ (up to 0.7055) and low $^{206}Pb/^{204}Pb$ (down to 17.3), apparently from assimilation of early Tertiary sediment and basic lower crustal rocks of Late Proterozoic age [25]. Detailed chemical information on the earlier picrites of the Anaanaa Member is not yet available. Crustal contamination alone cannot explain the systematic major-, trace-element and isotopic variations seen in the picrites of the Vaigat Formation [17]. In addition to a plume source, it appears that some MORB mantle was involved in the origin of these picrites, and its influence decreased with time going from earlier parts of the Naujánguit Member to the Ordlingassoq Member [17,21].

2. Methods

2.1. Helium isotope analysis

Olivine phenocrysts were concentrated from crushed rocks by sieving and magnetic separation, and hand-picked under a binocular microscope. Grains were ultrasonically cleaned in deionized water, then in acetone and air-dried, and reinspected under the microscope. Phenocrysts showing adhering rock matrix or any signs of alteration were rejected. Olivine separates were first analyzed by in vacuo crushing to liberate gases trapped within melt and/or fluid inclusions. This was done by loading the sample into a stainless steel chamber together with a magnetic piston, then lifting and dropping the piston about 150 times under vacuum using a system of external solenoids. The sample was crushed to a powder while still connected to the vacuum line. Non-condensable, reactive gases were gettered over hot Ti, and the heavy rare gases Ar, Kr and Xe were trapped on activated charcoal using liquid N_2. Neon was separated onto a cryogenically controlled charcoal trap at 38 K. The helium was admitted directly to the mass spectrometer for isotope ratio and peak height determination.

The vacuum line blank for crushing is $<1 \times 10^{-10}$ ccSTP for ^{4}He. During the period in which these analyses were performed, line blanks were run before and after all samples. Several days before a batch of sample analyses was performed, SAES getters in the mass spec static volume were reactivated to improve hydrogen removal efficiency, and only line blanks and small gas standards were analyzed. This procedure helped to reduce the size and variability of the mass spec ^{4}He memory (which dominated the blank correction) due to the recent history of sample analyses. Adhering to this procedure was especially significant for this study, because the amount of ^{4}He in these samples is small, and the blank + memory contribution to ^{4}He is relatively large, but very stable. Samples were analyzed when uncertainties in the mean value of the blank + memory correction were below 3% (2σ). One of the West Greenland picrites (332788) was analyzed three times over the course of this study, including once through a stepwise crushing procedure. The He isotope results for this sample agree within analytical uncertainty (Tables 1 and 2).

Olivine powders remaining from the crushing were transferred to a high temperature vacuum furnace for determination of ^{3}He/^{4}He and [He] within the olivine lattice. Sample powders wrapped in Al-foil boats were dropped into the crucible and melted at ~1800ºC by resistive heating. The furnace is connected in parallel with the crushing system to the mass spectrometer sample gas processing line. The furnace blank at 1800ºC is $<5 \times 10^{-10}$ ccSTP ^{4}He.

Simultaneous measurement of ^{3}He and ^{4}He was performed on a double collector mass spectrometer especially designed for high precision helium analysis by one of us (J.E.L.). A brief description of the instrument and operational details have been given previously [27].

2.2. Pb, Nd and Sr isotope analysis

Pb isotopes were determined on whole rock powders following methods described previously [28]. The fraction containing alkalis and rare earth elements (REE) from the primary Pb column was saved for Sr and Nd separation. Sr was separated in a quartz glass column using cation exchange in an HCl medium. After Sr elution, Ba was removed with 2 M HNO_3 prior to eluting the REE with 6 M HNO_3. The Sr fraction was purified in a Teflon column using Eichrom Sr Spec resin with an HNO_3 medium. Nd was separated from the REE in a quartz glass column using Eichrom Ln Spec resin in HCl.

For the determination of Pb isotope composition (IC), approximately 1 g of whole rock powder was acid-washed in cold 2 M HCl, followed by a wash in 1 M HBr and finally a rinse in quartz-distilled H_2O. This procedure was found to remove about 40% of the total Pb (e.g. sample 332788 in Table 3) but not to cause significant change in Pb isotope compositions. The Pb, U and Th elemental abundances were determined on unleached powders by isotope dilution (ID) with a spike enriched in ^{208}Pb, ^{235}U, and ^{230}Th. Approximately 1 g of powder for ID analysis was decomposed in a mixture of HF–HNO_3–$HClO_4$ to ensure complete spike–sample equilibration. The ^{87}Sr/^{86}Sr ratio was found to decrease in two of the three samples where acid leaching was performed (332788 and 400457) by up to 0.0002, while in sample 362149 it remained unchanged. The ^{143}Nd/^{144}Nd ratio increased slightly, by up to

Table 1
Helium isotopes for olivine phenocrysts from West Greenland picrites

Sample	Lat. (°N)	Long. (°W)	Elevation (m)	Stratigraphic member & *type*	Crushed					Melted powder			
					size fraction (mm)	weight (mg)	$^3He/^4He$ (R/R_A)	$2\sigma_m$	[He] (10^{-9} ccSTP/g)	weight (mg)	$^3He/^4He$ (R/R_A)	$2\sigma_m$	[He] (10^{-9} ccSTP/g)
332828	70.2720	52.6396	1080	upper Ordlingassoq *pillow breccia*	0.85–1.7	317.8	28.05	1.82	1.22 (5.3, 61.3)	304.6	0.54	0.04	33.02
332788	70.5000	53.6495	1370	lowermost Ordlingassoq *lava*	0.85–1.7	539.9	30.59	0.44	6.70 (0.3, 14.4)	490.9	4.17	0.06	36.26
				(replicate)	0.85–1.7	317.0	30.20	0.54	5.69 (0.4, 14.7)	302.5	4.13	0.07	41.11
362149	70.3694	53.2956	710	middle Nuajánguit *pillow breccia*	0.25–0.85	200.2	30.74	1.40	4.12 (2.1, 48.4)	190.8	0.67	0.04	42.01
362275	70.4150	53.8758	793	lower Nuajánguit *lava*	0.85–1.7	331.8	4.13	0.93	0.42 (37.2, 81.7)	311.6	4.60	0.15	12.98
400457	70.5184	54.1720	100	middle Anaanaa *lava*	0.25–0.85	309.8	17.55	2.00	0.71 (10.9, 77.8)	290.1	0.62	0.03	14.37

All values are blank corrected. Values in parentheses are the percentage of the measured ^3He and ^4He for each analysis that was due to the blank. Reported uncertainties in He isotope ratio represent the 2-sigma quadrature sum of the in-run ion counting uncertainties on the ^3He beam, plus uncertainties due to blank variability and reproducibility of air standards.

Table 2
Stepwise crushing experiment for olivine from sample 332788

Step Nr.	Nr. of strokes	$^3He/^4He$ (R/R_A)	$2\sigma_m$	He (10^{-9} ccSTP)
1	8	32.06	1.56	0.315
2	15	28.59	2.72	0.160
3	30	28.48	2.24	0.206
4	60	31.71	1.49	0.303
5	120	29.40	0.86	0.855
6	240	27.78	1.38	0.471
7	240	20.61	1.31	0.228
8	240	22.04	2.21	0.202

Sample weight 439.4 mg, size 0.25–0.85 mm. Total crushed [He] $= 6.23x10^{-9}$ ccSTP/g. Fusion of the powder after crushing gave $^3He/^4He = 1.28 \pm 0.03$ R_A, [He] $= 50.2x10^{-9}$ ccSTP/g.

0.00003 in the two samples analyzed for Nd where acid leaching was carried out (362149 and 400457; Table 3).

Pb, Nd and Sr isotopic analyses were performed on a VG-SECTOR 54 mass spectrometer. Analytical details are given in the footnote to Table 3.

3. Results and discussion

The most significant observation from this study is the high $^3He/^4He$, up to 31 R_A, in the gases released by crushing (Table 1). These values are comparable to those in young volcanic rocks from Loihi Seamount (up to 32 R_A; [29,30]), where the highest volcanic $^3He/^4He$ ratios are found today. Magmatic $^3He/^4He$ ratios above 25 R_A have been found at only three hotspot localities, namely Hawaii, Samoa and Iceland [29–32]. Such high ratios are generally attributed to the presence of an upwelling mantle plume which carries deep mantle material toward the Earth's surface. The West Greenland picrites show high $^3He/^4He$ ratios throughout the Vaigat Formation. The highest values (28–31 R_A) occur in the

Table 3
Sr, Nd and Pb isotope compositions and Pb, U, Th concentrations for West Greenland picrites

Sample		$^{87}Sr/^{86}Sr$	$^{143}Nd/^{144}Nd$	$^{206}Pb/^{204}Pb$	$^{207}Pb/^{204}Pb$	$^{208}Pb/^{204}Pb$	[Pb] (ppb)	[U] (ppb)	[Th] (ppb)	$^{238}U/^{204}Pb$	$^{232}Th/^{238}U$
332828	leached	0.702975	0.513113	17.938	15.404	37.619	–	–	–	–	–
	unleached	–	–	–	–	–	378	48.2	151	7.93	3.24
332788	leached	0.703478	0.512974	18.105	15.482	38.034	444	–	–	–	–
	unleached	0.703619	–	18.103	15.458	37.994	681	105	456	9.73	4.47
	leachate	–	–	18.201	15.463	38.164	–	–	–	–	–
362149	leached	0.703027	0.513114	17.972	15.410	37.760	–	–	–	–	–
	unleached	0.703026	0.513084	17.964	15.423	37.750	359	61.5	208	10.7	3.50
362275	leached	0.703147	–	17.740	15.399	37.573	–	–	–	–	-
	unleached	–	–	–	–	–	282	43.1	136	9.48	3.26
400457	leached	0.703077	0.513151	17.813	15.393	37.505	–	–	–	–	–
	unleached	0.703277	0.513125	17.821	15.384	37.499	347	38.5	106	6.89	2.84

Isotope analyses were performed on a VG-SECTOR 54 mass spectrometer. Samples were analyzed as metal species. Pb was loaded on a loop type Re filament with silica gel and phosphoric acid, and data were collected in static mode. Raw data were corrected for mass fractionation and machine bias based on replicate analyses of NIST SRM981 for Pb (using the values of Todt et al. [70]) and of NIST U050 for U and Th. Mass discrimination for Pb averaged $0.0687 \pm 0.0249\%$ ($2\sigma_m$) per mass unit. Total uncertainties in the Pb isotope ratios are <0.05% per amu, computed by error propagation of both sample and standard analyses. The Pb blanks were <100 pg for the IC and <150 pg for the ID procedures, and are negligible. Uncertainties for U, Th and Pb concentrations are <1% ($2\sigma_m$) in all cases. Sr was loaded on a loop type filament with a slurry of Ta_2O_5 in phosphoric acid, and data were collected in multi-dynamic mode. Repeated measurements of $^{87}Sr/^{86}Sr$ for NIST SRM987 at SDSU gave 0.710273 ± 0.000003 ($2\sigma_m$, $n = 78$); sample measurements have been normalized to $^{88}Sr/^{86}Sr = 0.1194$ and referenced to a value of 0.71025 for the standard. Nd was loaded with an HCl–phosphoric acid mixture onto a Re side filament using the triple filament technique, and data were collected in multi-dynamic mode. Repeated measurements of $^{143}Nd/^{144}Nd$ for the La Jolla Nd standard gave 0.511841 ± 0.000002 ($2\sigma_m$, $n = 41$); sample measurements have been normalized to $^{146}Nd/^{144}Nd = 0.7219$ and referenced to a value of 0.511858 for the standard. Procedural blanks for Sr and Nd are <50 pg and are negligible for the analyses reported here.

upper Naujánguit Member and throughout the Ordlingassoq Member, but a high $^3He/^4He$ ratio of 17.5 R_A is also present in the deeper Anaanaa Member. The high $^3He/^4He$ ratios measured here provide strong evidence for the presence of Iceland plume material beneath West Greenland at 61 Ma.

The helium contents of these olivine samples are low and lie between (0.7 and 6.7) $\times 10^{-9}$ ccSTP/g. These concentrations are well below the arbitrary cutoff of Hilton et al. [33] of 40×10^{-9} ccSTP/g, below which they suggested that $^3He/^4He$ ratios of ocean island basalt phenocrysts may be compromised by shallow level contamination with radiogenic helium. This has clearly not been the case for the West Greenland picrites.

3.1. Cosmogenic, radiogenic and nucleogenic He in old rocks

The potential presence of cosmogenic ^3He needs to be evaluated whenever old samples show elevated $^3He/^4He$ ratios. Rocks exposed at the Earth's surface for significant time periods may acquire higher $^3He/^4He$ ratios, chiefly through spallation reactions involving cosmic ray secondary particles with target nuclides of Si, O and Mg [34,35]. The cosmic ray secondaries are strongly attenuated in the atmosphere, and the ^3He production rate increases nearly exponentially with atmospheric height. Samples taken from near sea level, if exposed for only a few tens of thousands of years during active erosion, will not have a significant component of cosmogenic helium, while samples exposed at higher elevations may witness much higher production rates.

The last glacial maximum in Greenland occurred 30,000–15,000 years ago [36]. Approximately 8000–10,000 years ago, rapid glacial recession took place and left the area much the way it is now. In the northern parts of West Greenland, the main glaciers were confined to valleys and did not cover the higher elevations [37], although local glaciers may have been considerably higher, as they are today. For western Nuussuaq, the level representing the height of the main valley-filling glaciers is estimated at ~400 m elevation. Consequently, Nuussuaq samples collected above 400 m, from areas of slow erosion, may have been exposed since before the last stage of glaciation and possibly since before 100,000 years ago (A. Weidick, pers. commun.). At that time the whole area was certainly glacially covered, as evidenced by gneiss boulders on some mountain tops. Samples studied here were collected between 100 m and 1370 m elevation (Table 1). All of them except the Anaanaa lava (sample 400457) lie above ~400 m elevation. However, sample 332828 was taken from the foot of a steep breccia wall in a cirque which must have held a corrie glacier, and which must have undergone significant erosion during the most recent glaciation. Therefore, samples 400457 and 332828 have likely been exposed for $<$6000 years. For the remaining samples, a potential cosmogenic helium signature cannot be ruled out on the basis of field evidence alone.

The amount of ^3He released by crushing of the picrite olivines is relatively small, and if it was attributable to cosmogenic production then it would require relatively short exposure times. For example, sample 332788 has the highest crushed [^3He] of 2.9×10^{-13} ccSTP/g ($\sim 8 \times 10^6$ atoms), which at an elevation of 1370 m (cosmogenic ^3He production rate of ~380 atoms/year) could be produced in about 20,000 years. In young basalts, cosmogenic ^3He is generally confined to the crystal lattice, and the helium trapped in melt and/or fluid inclusions seems little affected by its presence [34]. Volatiles trapped in phenocrysts appear to be primarily contained in fluid inclusions that form within melt inclusions due to differential shrinkage upon cooling [38]. It is possible that diffusive exchange between cosmogenic He produced in glassy melt inclusions and the original He trapped in fluid inclusions might lead to an enhancement of cosmogenic He in the fluid phase. However, if this were the case, one would expect an inverse relationship between crushed He contents and $^3He/^4He$ ratios, because the cosmogenic (high ^3He) component would be more easily discernible when the trapped (high ^4He) component was less. Such a relationship is not present in the West Greenland picrites, and in fact, lower $^3He/^4He$ ratios occur at lower trapped He contents (Table 1). Based on these observations, and by analogy with young basalts, we hypothesize that crushing has selectively released only magmatic helium in the West Greenland picrites.

The issue of cosmogenic He in old rocks may be examined in more detail through fusion analysis

of the crushed powders. If the fusion yields a much lower $^3He/^4He$ ratio then the lattice contains dominantly radiogenic helium, from post-eruptive, in situ radioactive decay of U and Th or from α-particle implantation by the surrounding host rock. Our melted powder results show much lower $^3He/^4He$ ratios and high ^4He contents upon melting. Sample 362275 is an exception because it also showed a low $^3He/^4He$ ratio upon crushing (4.1 R_A). The low value for this sample seems unlikely to represent the magmatic value, because this sample also has the lowest crushed He concentration (0.4 nccSTP/g). In thin section this sample shows signs of cataclasis and its matrix clearly shows the most coarse-grained texture of any sample studied (see **EPSL Online Background** [2]), suggesting that it underwent cooling at a significantly slower rate. Also, the equivalent $^3He/^4He$ ratio for both the crushing and melting analysis (4.1±0.9 vs. 4.6±0.2 R_A) indicates that any remaining trapped helium has re-equilibrated with post-eruptive radiogenic helium. For these reasons the crushed He isotope results for sample 362275 cannot be considered representative of the inherited $^3He/^4He$ at the time of eruption.

A significant degree of helium isotope disequilibrium is present within the olivine phenocrysts of the other four samples, with lower $^3He/^4He$ in the lattice (Table 1). The $^3He/^4He$ ratios in the lattice of these olivines range down to 0.5 R_A upon fusion of the crushed powders. These low ratios imply significant post-eruptive production of radiogenic ^4He. The amount of post-eruptive radiogenic helium is:

$$^4He^* = [^4He]_{melt}\left(1 - \frac{R_{melt}}{R_{crush}}\right)$$

where $[^4He]_{melt}$ is the helium concentration measured for the melted powder, R is the $^3He/^4He$ ratio, and isotopic equilibrium at the time of eruption between helium trapped in inclusions and within the lattice is assumed [39]. In the case of the two Ordlingassoq lavas, similar amounts of radiogenic helium are present when calculated by this method (32 nccSTP/g) despite their different sample localities, and their different $^3He/^4He$ ratios and amounts of helium released by melting. This further suggests

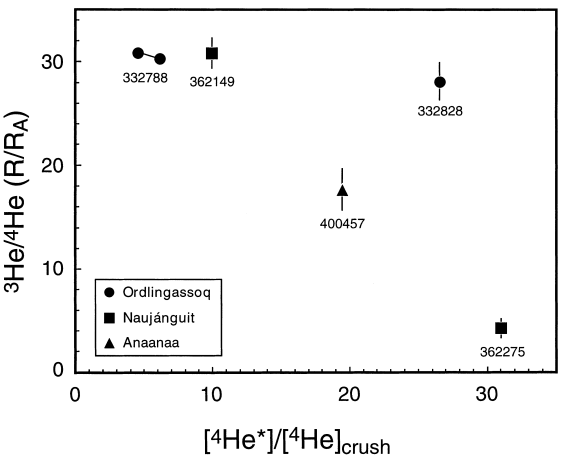

Fig. 2. The ratio of $^3He/^4He$ (expressed as R/R_A, i.e. relative to the atmospheric value) for gas released by crushing olivine phenocrysts vs. the ratio $^4He^*/[^4He]_{crush}$ measured for the same samples. $^4He^*$ is the amount of radiogenic He within the crystal lattice that was produced by radioactive decay of U and Th since the lava crystallized, and includes α-particles implanted from nearby U and Th decay in the host lava. Determination of $^4He^*$ rests on the assumption that isotope disequilibrium between He trapped in fluid/melt inclusions (released by crushing) and He within the crystal lattice (released by melting of powders remaining after crushing) results from radioactive decay since the time of eruption. The wide range in the ratio of $^4He^*/[^4He]_{crush}$ (5 to 27) at high ratios of $(^3He/^4He)_{crush}$ for three of the samples suggests that the crushing measurements accurately record the magmatic $^3He/^4He$ ratio at the time of eruption. Sample 362275 showed a low $^3He/^4He$ but no significant isotope disequilibrium between crushing and melting, and only an upper limit can be determined for its $^4He^*$, which is taken to be the amount of He released by melting of the crushed powder. The low $^3He/^4He$ ratio of this sample is most likely due to post-eruptive re-equilibration between trapped and radiogenic helium.

that the helium released during powder fusion is simply a binary mixture of inherited and radiogenic helium, and that cosmogenic ^3He production played a minor (if any) role in the origin of the crushed high $^3He/^4He$ ratios. The relative uniformity of the highest ratios at ∼30 R_A, for lavas from both the Ordlingassoq and Naujánguit members which show a wide range in $^4He^*$ (Fig. 2), also suggests that these very high $^3He/^4He$ ratios represent accurate estimates of the magmatic value at the time of lava emplacement, rather than minimum estimates as a result of preferential ^3He loss or small additions of radiogenic ^4He (which would be expected to produce significant inter-sample variability).

[2] http://www.elsevier.nl/locate/epsl,
mirror site: http://www.elsevier.com/locate/epsl

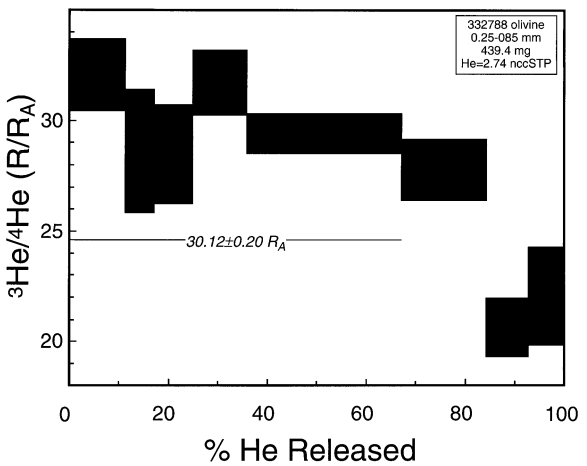

Fig. 3. $^3He/^4He$ vs. the percentage of He released by incremental crushing of olivine from picrite sample 332788. The weighted mean of the first five steps is 30.12 ± 0.20 R_A (2σ). This mean value (μ), weighted inversely to the analytical error (σ_i) associated with $^3He/^4He$ for each step (x_i), is given by [69] $\mu = [\Sigma(x_i/\sigma_i^2)]/[\Sigma(1/\sigma_i^2)]$.

A further means of evaluating high $^3He/^4He$ ratios in old samples may be through stepwise crushing (Fig. 3). When cosmogenic He is present in phenocrysts from young basalts it can be selectively extracted by low temperature heating of crushed phenocryst powders [40], suggesting that it is somewhat more 'loosely bound' in the crystal. In older samples, however, radiogenic He is also selectively released from phenocryst powders at low temperature [41,42], and this could obscure the presence of any cosmogenic helium released by a step heating experiment. Sample 332788, the sample with the highest olivine He content, was therefore analyzed by stepwise crushing to gain more insight into this question. Olivine from this sample was crushed incrementally by increasing the number of crushing strokes for each increment (Table 2). The first five steps released gas which had the same $^3He/^4He$ ratio within analytical uncertainty, after which the ratio began to decrease. The slight decrease of $^3He/^4He$ over the course of the procedure appears to indicate that small amounts of radiogenic helium were released in the last few steps. The mean of the first five crushing steps weighted inversely to their analytical uncertainties shows $^3He/^4He = 30.12 \pm 0.20$ R_A, in agreement with the single-stage extractions for this sample (Table 1). Our stepwise crushing extraction shows lower $^3He/^4He$ in the later steps, not higher values, which can also be taken as circumstantial evidence that a significant cosmogenic component is absent in this sample.

Finally, some ^3He may be produced within a crystal by neutron capture via the reaction $^6Li(n,\alpha)^3H \rightarrow {}^3He$, where the neutrons result from α-particle interactions with light element nuclei in the rock [43,44]. Approximately 2.5 neutrons are produced per million α-particles in igneous rocks [44]. If we take the ^4He content in the olivine from sample 332788 as an upper limit to the time-integrated α-particle flux, this gives 10^{12} atoms of ^4He per gram, and an integrated neutron flux (Φ) of 2.5×10^6 neutrons per gram (5.3×10^6 n/cm^2 for cubic geometry and density of 3.3). The Li content of olivine is typically around 2 ppm (1.7×10^{17} atom/g) [45], and the neutron capture cross-section for Li decay by α-particle emission (σ_{Li}) is 940 barns (940×10^{-24} cm^2) [46]. The production of ^3He is $J = Li \cdot \sigma_{Li} \cdot \Phi$, which in this case gives $^3He = 3.3 \times 10^{-17}$ ccSTP/g, a trivial amount compared to that measured ($^3He > 10^{-13}$ ccSTP/g). An alternative calculation can be made from the U and Th content of the whole rocks (Table 3). For the highest U and Th values measured (105 and 460 ppb), 4.2×10^{13} α-particles are produced in 60 million years. This still only translates to a ^3He production of 1.4×10^{-15} ccSTP/g. Although other reactions are possible, such as neutron production through muon capture [34], these are less important than the nucleogenic production of ^3He linked to radiogenic ^4He production. We conclude that nucleogenic production of ^3He plays no significant role in the case of the West Greenland picrites, consistent with our fusion results that approach the radiogenic production ratio for minerals of low Li content ($^3He/^4He \leq 0.1$ R_A).

3.2. The Iceland mantle plume at 60 Ma

In Pb isotopes, the West Greenland picrites closely resemble those lavas from the Faeroe Islands which are not crustally contaminated [47]. In Pb, Sr and Nd isotopes they are also similar to some Icelandic picrites and basalts, and show a marked resemblance to the Theistareykir picrites [48,49], except for sample 332788 which more closely re-

sembles lavas from the Reykjanes Peninsula [49–52].

Helium isotopes for the West Greenland picrites are shown against $^{87}Sr/^{86}Sr$, $^{143}Nd/^{144}Nd$, $^{206}Pb/^{204}Pb$ and $^{208}Pb^{*}/^{206}Pb^{*}$ in Fig. 4, where they are compared to volcanic rocks from ocean islands, the Mid-Atlantic Ridge, and some continental regions. The $^{208}Pb^{*}/^{206}Pb^{*}$ is the isotopic ratio corrected for primordial Pb, and is related to the time-integrated Th/U ratio [53]. The points shown in Fig. 4 for the West Greenland picrites are measured ratios for the acid-leached powders uncorrected for their age, but the age corrections are relatively small. For Pb isotopes, the ranges in μ ($^{238}U/^{204}Pb$) are 6.9–10.7 and in κ ($^{232}Th/^{238}U$) are 2.8–4.5 (Table 3). Based on these ratios, the initial values of $^{206}Pb/^{204}Pb$, $^{207}Pb/^{204}Pb$ and $^{208}Pb/^{204}Pb$ at 60 Ma would have been lower by 0.06–0.10, 0.003–0.005 and 0.06–0.14, respectively. These changes are slightly larger than the analytical uncertainties for $^{206}Pb/^{204}Pb$ and $^{208}Pb/^{204}Pb$. In the cases of Sr and Nd we can estimate the initial isotope ratios assuming that Rb/Sr and Sm/Nd ratios previously reported for other West Greenland picrites are appropriate [17]. For the Ordlingassoq picrites, the maximum effect can be calculated from the highest Rb/Sr and Sm/Nd, which are 0.0136 and 0.318, respectively. These cause initial $^{87}Sr/^{86}Sr$ to be lower by 0.00003 and initial $^{143}Nd/^{144}Nd$ by 0.00008. These differences are also significant compared to analytical uncertainty, especially for Nd. However, the measured parent–daughter ratios should follow those in the mantle source given that picrites are formed by relatively large degrees of melting, and this effect serves to decrease the isotopic discrepancies. For example, the above Sm/Nd corresponds to a change in ε_{Nd} of only 0.03 units in 60 million years. For the purpose of making comparisons to the mantle sources of oceanic basalts, we take the measured isotopic compositions of West Greenland picrites to represent mantle source values.

Even though the highest $^{3}He/^{4}He$ ratios nearly overlap, there does appear to be some covariation between He and the other isotope systems. If the data in Fig. 4 are viewed from the standpoint of mixing between plume and depleted mantle end-members, it would suggest that the plume end-member is relatively enriched in ^{3}He compared to either ^{86}Sr, ^{144}Nd or ^{204}Pb, as expected for material with a deep mantle origin. In detail, because the highest $^{3}He/^{4}He$ ratios are similar, this interpretation rests on the dispersion in Sr, Nd and Pb isotopes, and on the isotope composition of the single Anaanaa picrite with lower $^{3}He/^{4}He$. The Anaanaa picrite appears to have the highest proportion of a depleted mantle end-member in terms of He, Pb and Nd isotopes, although its $^{87}Sr/^{86}Sr$ overlaps with the Ordlingassoq and Naujánguit lavas with very high $^{3}He/^{4}He$ (Fig. 4). The uniformity of the highest $^{3}He/^{4}He$ values despite some dispersion in the other isotopes supports our contention that the crushing results accurately represent the original magmatic $^{3}He/^{4}He$ at the time of eruption. Based on the results shown in Fig. 4, the Iceland mantle plume source at 60 Ma appears unlikely to have had a $^{3}He/^{4}He$ ratio significantly higher than 30–35 R_A. The similarity of this $^{3}He/^{4}He$ ratio to the highest values measured today at oceanic hotspots is also rather striking. It suggests that deep mantle regions with $^{3}He/^{4}He$ much higher than 30–35 R_A are unlikely to have been present over the last ~100 million years of Earth history. These deep mantle regions appear to have κ_{Pb} values near 3.9–4.0 (Fig. 4D), consistent with a long-term history of quasi-isolation. Such inferred κ_{Pb} values resemble those for high-$^{3}He/^{4}He$ tholeiites from Hawaiian shield volcanoes, where a remarkable, internally consistent relationship between $^{3}He/^{4}He$ and $^{208}Pb/^{206}Pb$ has been found [54].

The onset of flood volcanism in both West and southeast Greenland was essentially synchronous at 61 Ma [11,12], and slightly older volcanism dated at 62 to 63 Ma occurred in the Hebrides [10]. There is still some debate about the precise location of the center of the Iceland plume at this time. White and McKenzie [55] place the axis of the plume at 61 Ma beneath eastern Greenland, approximately 900 km to the east of the Nuussuaq Peninsula, while Lawver and Müller [56] place it in central Greenland about 350 km to the northeast. In either case, a problem lies in explaining the occurrence in West Greenland of high temperature picrites associated with the arrival of the Iceland plume beneath the old, cratonic lithosphere of Greenland. In the standard flood basalt models the head of a rising plume spreads out laterally to a diameter of ~2000 km when it reaches

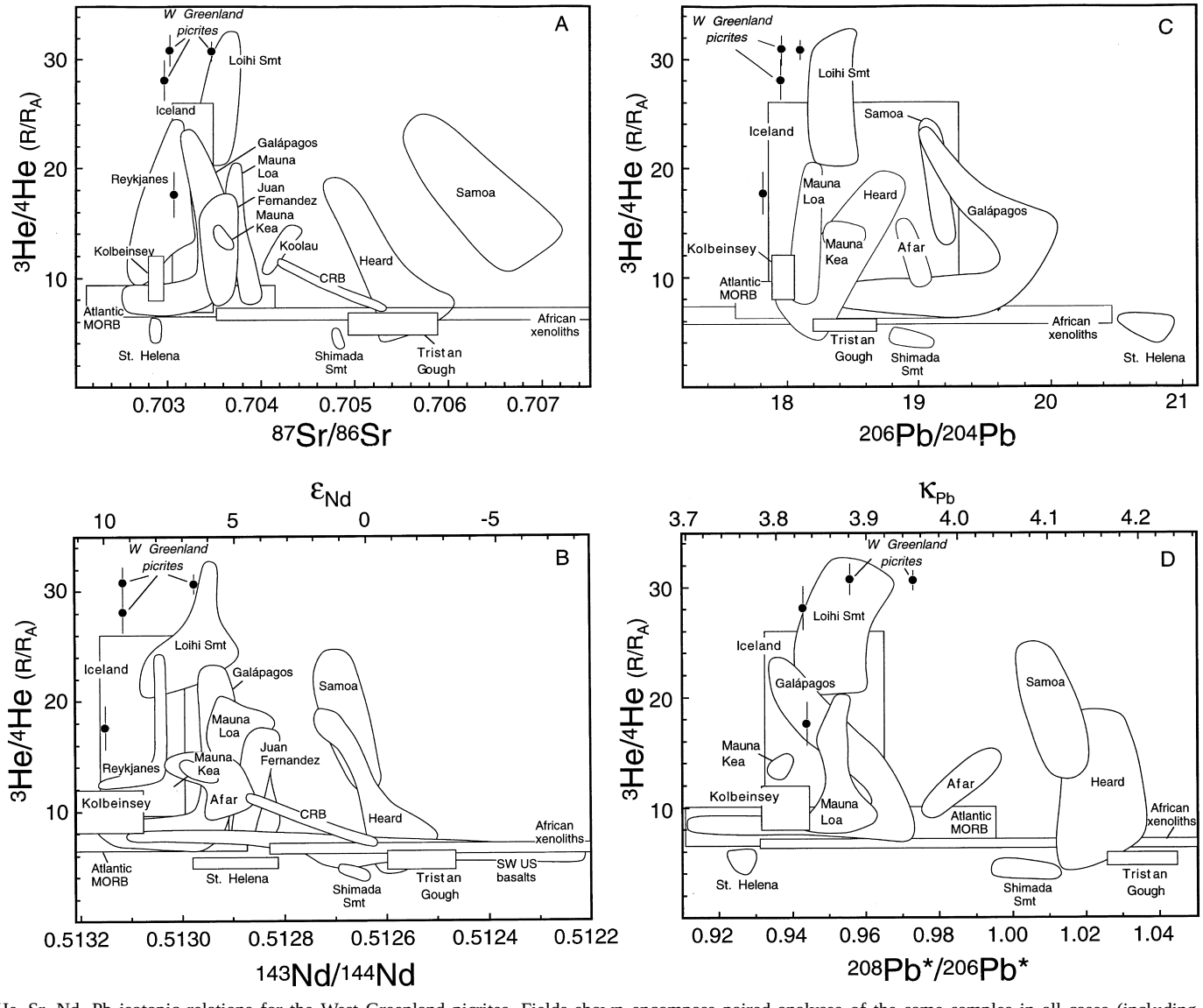

Fig. 4. He–Sr, Nd, Pb isotopic relations for the West Greenland picrites. Fields shown encompass paired analyses of the same samples in all cases (including MORB), except that where boxes are shown they encompass the range of values at those localities. Data sources are from the literature. (A) $^{3}He/^{4}He$ vs. $^{87}Sr/^{86}Sr$. (B) $^{3}He/^{4}He$ vs. $^{143}Nd/^{144}Nd$. (C) $^{3}He/^{4}He$ vs. $^{206}Pb/^{204}Pb$. (D) $^{3}He/^{4}He$ vs. $^{208}Pb^{*}/^{206}Pb^{*}$.

shallow mantle depths [55,57] and encounters the lithosphere. According to these models, the hottest mantle temperatures occur near the plume axis, and consequently, picrites and magnesian basalts should be found in these areas. Picrite eruptions at the periphery of the plume are not predicted by these models, as recognized earlier [15,26].

This problem may be reconciled by two different, though not mutually exclusive explanations. In the first explanation, previously suggested in part by Holm et al. [17] and Larsen et al. [20], the rising Iceland plume may have been 'split' at depth by the underside topography of the Greenland craton protruding into the upper mantle. If the plume axis was wide, as it appears beneath Iceland today (~300 km) from seismic tomography [58], then hot, picritic magmas might be produced at significant lateral distances away from the center of plume impact due to such lithospheric deflection. It is noteworthy that the Iceland plume currently has a somewhat tapered shape [58], and that picrites in Iceland, such as from Theistareykir and the Reykjanes Peninsula, also occur near the edges of this upwelling zone along areas of active extension. This situation must allow hot and deep magmas such as picrites to ascend rapidly to the surface [26]. A second explanation for the location of the West Greenland picrites calls upon rapid lateral channeling of hot plume head material in the shallow mantle without significant cooling. Recent numerical models of plume ascent and dispersal of starting plume head material that include non-Newtonian, temperature- and depth-dependent rheology predict ultra-fast vertical and lateral flow rates of 1 to 10 m/year for hot plume material [59,60]. These high dispersal rates could account for nearly simultaneous volcanism in West and southeast Greenland associated with plume impact [11]. The delay of 1 to 2 million years in the eruption of the Vaigat picrites compared to lavas in the Hebrides could reflect the duration of lateral plume flow in the upper mantle at these very high rates. Non-Newtonian rheology can also affect the distribution of melting anomalies associated with fast-spreading plume material, because rapid bursts of viscous heating can produce localized zones having very high temperatures [61]. These hot zones may represent the sources for picritic magmas such as those erupted in West Greenland.

3.3. Helium isotope evolution of the deep mantle

Large igneous provinces are widely accepted to reflect some contribution from mantle plumes (e.g. [55,57,62,63]), although the style of upwelling and its role in driving extension and mantle melting are debated among the plume models. A few proponents for a non-plume origin remain (e.g. [64,65]), and they generally rely upon models of voluminous magmatism focused at rifted continental margins due to an enhanced thermal contrast between cold, cratonic lithosphere and warm upper mantle. Our high $^3He/^4He$ results bear on a choice between these alternatives. If such high $^3He/^4He$ ratios represent an origin from the deep mantle (e.g. [1–4]), then models for flood basalt volcanism in the absence of a mantle plume are not tenable.

Mantle plumes could have operated throughout most of Earth history at their present level of intensity [66], and some picrites and komatiites may represent a nearly direct sampling of the deeper mantle. Campbell and Griffiths [67] pointed out a major change in the character of komatiites and picrites near the Archean–Proterozoic boundary. In earlier times these rock types show more depleted chemistry and have higher MgO (typically >30%), whereas in the Proterozoic and later times most of them show a more enriched character resembling ocean island basalts and have lower MgO (<22%). This change is probably due to changes in convective style of the Earth's mantle, and the increased importance of thermo-regulation by slab subduction and volatile recycling with time [66,68]. The existence of high $^3He/^4He$ in at least two cases of old, high MgO lavas (39 R_A in the 2.7 Ga komatiites of Alexo, Ontario [8] and 30 R_A in the 61 Ma picrites of West Greenland) indicates that, with further work, it may be possible to better constrain the thermal evolution of the deep mantle from $^3He/^4He$ studies of picrites and komatiites associated with large igneous provinces.

4. Summary

Picrites from the 61 Ma Vaigat Formation of West Greenland show $^3He/^4He$ ratios trapped in olivine phenocrysts which range up to 30 times the atmospheric ratio. These high values represent a well-pre-

served magmatic signature attributed to the presence of the early Iceland plume during flood basalt volcanism in the North Atlantic. The picrites studied here show Pb isotope compositions that resemble those for the least contaminated basalts from the Faeroe Islands. Their Pb, Nd and Sr isotope compositions are also similar to recent Icelandic picrites from Theistareykir and the Reykjanes Peninsula. Helium isotopes in the West Greenland picrites show a general covariation with Pb, Nd and Sr isotopes that can be explained by mixing between a high-$^3He/^4He$ plume source and a depleted (MORB) mantle source, or by isotopic heterogeneity within the plume itself. The high $^3He/^4He$ ratios, along with the synchroneity of magmatism across the North Atlantic Volcanic Province at 60–62 Ma, suggest very rapid dispersion of hot, plume head material in the shallow mantle during the early stages of plume impact.

The observation of initial $^3He/^4He$ ratios in picrites from West Greenland that are as high as any values at young hotspots improves the outlook for He isotope studies over the 10^8 year lifetime of large mantle plumes. If the problems of radiogenic, cosmogenic and nucleogenic additions can be adequately dealt with in ancient samples, then He isotope work on well-preserved picrites and komatiites may aid in reconstructing the thermal and geochemical evolution of the deep mantle.

5. Note added in proof

Work carried out by Marty et al. [71] at the same time as this study, shows the $^3He/^4He$ ratios up to 21 R_A in the Hold with Hope area of northeast Greenland at 58 Ma, further evidence for the very high $^3He/^4He$ character of the early Iceland mantle plume.

Acknowledgements

We thank Anker Weidick, Bob Duncan and Peter Meyer for helpful discussions. We also thank Ken Farley and two anonymous reviewers for constructive comments that improved the manuscript. The helium isotope mass spectrometer facility was supported by the NOAA Vents Program; other support for the analytical work was provided by the Ocean Sciences Division of NSF. Publication of the results has been authorized by the Geological Survey of Denmark and Greenland. ***[FA]***

References

[1] M.D. Kurz, W.J. Jenkins, S.R. Hart, Helium isotopic systematics of oceanic islands and mantle heterogeneity, Nature 297 (1982) 43–46.

[2] C.J. Allègre, T. Staudacher, P. Sarda, M. Kurz, Constraints on evolution of Earth's mantle from rare gas systematics, Nature 303 (1983) 762–766.

[3] L.H. Kellogg, G.J. Wasserburg, The role of plumes in mantle helium fluxes, Earth Planet. Sci. Lett. 99 (1990) 276–289.

[4] R.K. O'Nions, I.N. Tolstikhin, Limits on the mass flux between lower and upper mantle and stability of layering, Earth Planet. Sci. Lett. 139 (1996) 213–222.

[5] A.R. Basu, P.R. Renne, D.K. Das Gupta, F. Teichmann, R.J. Poreda, Early and late alkali igneous pulses and a high ^3He plume origin for the Deccan flood basalts, Science 261 (1993) 902–906.

[6] A.R. Basu, R.J. Poreda, P.R. Renne, F. Teichmann, Y.R. Vasiliev, N.V. Sobolev, B.D. Turrin, High-^3He plume origin and temporal–spatial evolution of the Siberian flood basalts, Science 269 (1995) 822–825.

[7] B. Marty, R. Pik, G. Yirgu, Helium isotopic variations in Ethiopian plume lavas: nature of magmatic sources and limit on lower mantle contribution, Earth Planet. Sci. Lett. 144 (1996) 223–237.

[8] D. Richard, B. Marty, M. Chaussidon, N. Arndt, Helium isotopic evidence for a lower mantle component in depleted Archean komatiite, Science 273 (1996) 93–95.

[9] A. Dodson, B.M. Kennedy, D.J. DePaolo, Helium and neon isotopes in the Imnaha Basalt, Columbia River Basalt Group: evidence for a Yellowstone plume source, Earth Planet. Sci. Lett. 150 (1997) 443–451.

[10] D.G. Pearson, C.H. Emeleus, S.P. Kelley, Precise $^{40}Ar/^{39}Ar$ ages for the initiation of igneous activity in the Small Isles, Inner Hebrides and implications for the timing of magmatism in the British Tertiary Volcanic Province, J. Geol. Soc. London 153 (1996) 815–818.

[11] M. Storey, R.A. Duncan, A.K. Pedersen, L.M. Larsen, H.C. Larsen, $^{40}Ar/^{39}Ar$ geochronology of the West Greenland Tertiary volcanic province, Earth Planet. Sci. Lett. (1998) in press.

[12] C.W. Sinton, R.A. Duncan, ^{40}Ar–^{39}Ar ages of lavas from the southeast Greenland margin, ODP Leg 152 and the Rockall Plateau, DSDP Leg 81, Proc. ODP Sci. Res. 152 (1998) in press.

[13] A.D. Saunders, J.G. Fitton, M.J. Norry, R.W. Kent, The North Atlantic Igneous Province, in: J.J. Mahoney, M.F. Coffin (Eds.), Large Igneous Provinces, AGU Monogr. 109 (1997) 45–93.

[14] R.S. White, A hot-spot model for early Tertiary volcanism in the N Atlantic, in: A.C. Morton, L.M. Parson (Eds.), Early Tertiary Volcanism and the Opening of the NE Atlantic, Geol. Soc. London Spec. Publ. 39 (1988) 3–13.
[15] J.A. Chalmers, L.M. Larsen, A.K. Pedersen, Widespread Paleocene volcanism around the northern North Atlantic and Labrador Sea: evidence for a large, hot, early plume head, J. Geol. Soc. London 152 (1995) 965–969.
[16] P.M. Holm, N. Hald, T.F. Nielsen, Contrasts in composition and evolution of Tertiary CFBs between West and East Greenland and their relations to the establishment of the Icelandic mantle plume, in: B.C. Storey, T. Alabaster, R.J. Pankhurst (Eds.), Magmatism and the Causes of Continental Break-up, Geol. Soc. London Spec. Publ. 68 (1992) 349–362.
[17] P.M. Holm, R.C.O. Gill, A.K. Pedersen, J.G. Larsen, N. Hald, T.F.D. Nielsen, M.F. Thirlwall, The Tertiary picrites of West Greenland: contributions from 'Icelandic' and other sources, Earth Planet. Sci. Lett. 115 (1993) 227–244.
[18] A.K. Pedersen, Reaction between picrite magma and continental crust: early Tertiary silicic basalts and magnesian andesites from Disko, West Greenland, Bull. Grønl. Geol. Unders. 152 (1985) 1–126.
[19] A.K. Pedersen, Lithostratigraphy of the Tertiary Vaigat Formation on Disko, central West Greenland, Rapp. Grønl. Geol. Unders. 124 (1985) 1–30.
[20] L.M. Larsen, A.K. Pedersen, G.K. Pedersen, S. Piasecki, Timing and duration of Early Tertiary volcanism in the North Atlantic: new evidence from West Greenland, in: B.C. Storey, T. Alabaster, R.J. Pankhurst (Eds.), Magmatism and the Causes of Continental Break-up, Geol. Soc. London Spec. Publ. 68 (1992) 321–333.
[21] L.M. Larsen, A.K. Pedersen, Earliest Tertiary break-up volcanism in West Greenland: Mg-rich volcanics from Nussuaq and Disko, J. Conf. Abstr. 1 (1996) 349.
[22] D.B. Clarke, A.K. Pedersen, Tertiary volcanic provinces of West Greenland, in: A. Escher, W.S. Watt (Eds.), The Geology of Greenland, The Geological Survey of Greenland, Copenhagen, 1976, pp. 364–385.
[23] L.M. Larsen, A.K. Pedersen, Volcanic marker horizons in the Maligât formation on Disko and Nûgssuaq, and implications for the development of the southern part of the west Greenland basin in the early Tertiary, Rapp. Grønl. Geol. Unders. 148 (1990) 65–73.
[24] P. Riisager, Magnetostratigraphy of Paleocene lavas from the Vaigat Formation of West Greenland, Geophys. J. Int. (1998) in press.
[25] P. Lightfoot, C.J. Hawkesworth, K. Olshefsky, T. Green, W. Doherty, R.R. Keays, Geochemistry of Tertiary tholeiites and picrites from Qerqertarssuaq (Disko Island) and Nuussuaq, West Greenland with implications for mineral potential of comagmatic intrusions, Contrib. Mineral. Petrol. 128 (1997) 139–163.
[26] R.C.O. Gill, A.K. Pedersen, J.G. Larsen, Tertiary picrites in West Greenland: melting at the periphery of a plume? in: B.C. Storey, T. Alabaster, R.J. Pankhurst (Eds.), Magmatism and the Causes of Continental Break-up, Geol. Soc. London Spec. Publ. 68 (1992) 335–348.
[27] D. Graham, J. Lupton, F. Albarède, M. Condomines, Extreme temporal homogeneity of helium isotopes at Piton de la Fournaise, Réunion Island, Nature 347 (1990) 545–548.
[28] B.B. Hanan, J.-G. Schilling, Easter microplate evolution: Pb isotope evidence, J. Geophys. Res. 94 (1989) 7432–7448.
[29] M.D. Kurz, W.J. Jenkins, S.R. Hart, D. Clague, Helium isotopic variations in the volcanic rocks from Loihi Seamount and the island of Hawaii, Earth Planet. Sci. Lett. 66 (1983) 388–406.
[30] W. Rison, H. Craig, Helium isotopes and mantle volatiles in Loihi Seamount and Hawaiian Island basalts and xenoliths, Earth Planet. Sci. Lett. 66 (1983) 407–426.
[31] M. Condomines, K. Gronvold, P.J. Hooker, K. Muehlenbachs, R.K. O'Nions, N. Oskarsson, E.R. Oxburgh, Helium, oxygen, strontium and neodymium isotopic relationships in Icelandic volcanics, Earth Planet. Sci. Lett. 66 (1983) 125–136.
[32] K.A. Farley, J.H. Natland, H. Craig, Binary mixing of enriched and undegassed (primitive?) mantle components (He, Sr, Nd, Pb) in Samoan lavas, Earth Planet. Sci. Lett. 111 (1992) 183–199.
[33] D.R. Hilton, J. Barling, G.E. Wheller, Effect of shallow-level contamination on the helium isotope systematics of ocean-island lavas, Nature 373 (1995) 330–333.
[34] M.D. Kurz, In situ production of terrestrial cosmogenic helium and some applications to geochronology, Geochim. Cosmochim. Acta 50 (1986) 2855–2862.
[35] D. Lal, Production of ^{3}He in terrestrial rocks, Chem. Geol. 66 (1987) 89–98.
[36] A. Weidick, Glaciation and the Quaternary, in: A. Escher, W.S. Watt (Eds.), The Geology of Greenland, The Geological Survey of Greenland, Copenhagen, 1976, pp. 431–458.
[37] S. Funder, L. Hansen, The Greenland ice sheet — a model for its culmination and decay during and after the last glacial maximum, Bull. Geol. Soc. Denm. 42 (1996) 137–152.
[38] E. Roedder, Fluid Inclusions, Mineralogical Society of America, Washington, DC, 1984, 644 pp.
[39] D.W. Graham, W.J. Jenkins, M.D. Kurz, R. Batiza, Helium isotope disequilibrium and geochronology of glassy submarine basalts, Nature 326 (1987) 384–386.
[40] M.D. Kurz, Cosmogenic helium in a terrestrial igneous rock, Nature 320 (1986) 435–439.
[41] D.W. Graham, S.E. Humphris, W.J. Jenkins, M.D. Kurz, Helium isotope geochemistry of some volcanic rocks from Saint Helena, Earth Planet. Sci. Lett. 110 (1992) 121–131.
[42] D.W. Graham, K.A. Hoernle, J.E. Lupton, H.-U. Schmincke, Helium isotope variations in volcanic rocks from the Canary Islands and Madeira, Chapman Conf., Shallow Level Processes in Ocean Island Magmatism: Distinguishing Mantle and Crustal Signatures, Puerto de la Cruz, Tenerife, 1996, pp. 13–14.
[43] L.T. Aldrich, A.O. Nier, The occurrence of ^{3}He in natural sources of helium, Phys. Rev. 74 (1948) 1590–1594.

[44] P. Morrison, J. Pine, Radiogenic origin of the helium isotopes in rock, Ann. N.Y. Acad. Sci. 62 (1955) 71–92.
[45] J.G. Ryan, C.H. Langmuir, The systematics of lithium abundances in young volcanic rocks, Geochim. Cosmochim. Acta 51 (1987) 1727–1741.
[46] R.B. Firestone, V.S. Shirley, Table of Isotopes, Vol. 1, Wiley Interscience, New York, 1996, 1531 pp.
[47] C. Gariépy, J. Ludden, C. Brooks, Isotopic and trace element constraints on the genesis of the Faeroe lava pile, Earth Planet. Sci. Lett. 63 (1983) 257–272.
[48] T. Elliott, C.J. Hawkesworth, K. Grönvold, Dynamic melting of the Iceland plume, Nature 351 (1991) 201–206.
[49] B.B. Hanan, J.-G. Schilling, The dynamic evolution of the Iceland mantle plume: the lead isotope perspective, Earth Planet. Sci. Lett. 151 (1997) 43–60.
[50] S.R. Hart, J.-G. Schilling, J.L. Powell, Basalts from Iceland and along the Reykjanes Ridge: Sr isotope geochemistry, Nat. Phys. Sci. 246 (155) (1973) 104–107.
[51] S.-S. Sun, M. Tatsumoto, J.-G. Schilling, Mantle plume mixing along the Reykjanes Ridge axis: Lead isotopic evidence, Science 190 (1975) 143–147.
[52] A. Zindler, S.R. Hart, F.A. Frey, S.P. Jakobsson, Nd and Sr isotope ratios and rare earth element abundances in Reykjanes Peninsula basalts: evidence for mantle heterogeneity beneath Iceland, Earth Planet. Sci. Lett. 45 (1979) 249–262.
[53] C.J. Allègre, B. Dupré, E. Lewin, Thorium/uranium ratio of the Earth, Chem. Geol. 56 (1986) 219–227.
[54] J. Eiler, K.A. Farley, E.M. Stolper, Correlated He and Pb isotope variations in Hawaiian lavas, Geochim. Cosmochim. Acta (1998) in press.
[55] R.S. White, D. McKenzie, Magmatism at rift zones: the generation of volcanic continental margins and flood basalts, J. Geophys. Res. 94 (1989) 7685–7729.
[56] L.A. Lawver, R.D. Müller, Iceland hotspot track, Geology 22 (1994) 311–314.
[57] I.H. Campbell, R.W. Griffiths, Implications of mantle plume structure for the evolution of flood basalts, Earth Planet. Sci. Lett. 99 (1990) 79–93.
[58] C.J. Wolfe, I.T. Bjarnason, J.C. VanDecar, S.C. Solomon, Seismic structure of the Iceland mantle plume, Nature 385 (1997) 247–247.
[59] T.B. Larsen, D.A. Yuen, Ultrafast upwelling bursting through the mantle, Earth Planet. Sci. Lett. 146 (1997) 393–400.
[60] P. van Keken, Evolution of starting mantle plumes: a comparison between numerical and laboratory models, Earth Planet. Sci. Lett. 148 (1997) 1–12.
[61] T.B. Larsen, D.A. Yuen, J.L. Smedsmo, A.V. Malevsky, Generation of fast timescale phenomena in thermo-mechanical processes, Phys. Earth Planet. Inter. 102 (1997) 213–222.
[62] R.W. Carlson, Physical and chemical evidence on the cause and source characteristics of flood basalt volcanism, Aust. J. Earth Sci. 38 (1991) 525–544.
[63] R.A. Duncan, M.A. Richards, Hotspots, mantle plumes, flood basalts and true polar wander, Rev. Geophys. 29 (1991) 31–50.
[64] J.C. Mutter, S.R. Buck, C.M. Zehnder, Convective partial melting, 1, A model for the formation of thick basaltic sequences during the initiation of spreading, J. Geophys. Res. 93 (1988) 1031–1048.
[65] S.D. King, D.L. Anderson, An alternative mechanism of flood basalt formation, Earth Planet. Sci. Lett. 136 (1995) 269–279.
[66] G.F. Davies, Conjectures on the thermal and tectonic evolution of the Earth, Lithos 30 (1993) 281–289.
[67] I.H. Campbell, R.W. Griffiths, The changing nature of mantle hotspots through time: implications of the geochemical evolution of the mantle, J. Geol. 92 (1992) 497–523.
[68] J. McGovern, G. Schubert, Thermal evolution of the Earth: effects of volatile exchange between atmosphere and interior, Earth Planet. Sci. Lett. 96 (1989) 27–37.
[69] P.R. Bevington, Data Reduction and Error Analysis for the Physical Sciences, McGraw-Hill, New York, 1969, 336 pp.
[70] W. Todt, R.A. Cliff, A. Hanser, A.W. Hofmann, $^{202}Pb + {}^{205}Pb$ double spike for lead isotopic analyses, Terra Cognita 4 (1984) 209.
[71] B. Marty, B.G.J. Upton, R.M. Ellam, Helium isotopes in early Tertiary basalts, northeast Greenland: evidence for 58 Ma plume activity in the North Atlantic-Iceland volcanic province, Geology 26 (1998) 407–410.

Field descriptions of sample locations and 'best estimates' for surface exposure times are provided below. Petrographic descriptions are also included, along with the range in Fo content for 10 olivine analyses from each sample. Olivine phenocryst compositions were analyzed with a Cameca SX-50 electron microprobe, using a beam current of 50 nA and accelerating voltage of 15 kV. Calibration was made through an Fo90 olivine standard, analyzed before and after each sample.

GGU 332828 70.27195°N, 52.6396°W, 1080 m elevation

A pillow breccia sample taken at the foot of a steep, eastern wall of a small cirque valley at Paatuut Puiattua. The cirque wall consists of fresh pillow breccias and pahoehoe lava flows from the upper part of the Ordlingassoq Member. This cirque was probably glacier filled during the last glaciation. Although the time of deglaciation is unknown, recent erosion has been significant, suggesting a short exposure time.

Olivine composition - Fo82.0-86.9. Abundant subhedral olivine phenocrysts and glomerocrysts up to 3 mm, containing spinel and glassy melt inclusions, along with olivine microphenocrysts and plagioclase laths up to 0.4 mm set in a hyalopilitic groundmass of plagioclase microlites, cryptocrystalline olivine, clinopyroxene, opaques and interstitial glass.

GGU 332788 70.50000°N, 53.6495°W, 1370 m elevation

A lava sample from Ukallit mountain (1440 m) at SE side of the wide Qunnilik valley. This mountain side, with trap topography, consists of 10-20 m thick massive subaerial lava flows. The sample was taken from the second flow in the Ordlingassoq Member, 0.7 m above the base of a 15 m-thick olivine-rich, crumbling, vesicular lava flow. This area was not ice covered during the last glaciation. There has been fresh erosion in the area, but the sample may have been exposed at the surface for several thousand years.

Olivine composition - Fo88.4-91.5. Abundant euhedral olivine phenocrysts containing spinel inclusions, subhedral olivine phenocrysts which occasionally exhibit strain lamellae, olivine glomerocrysts up to 6 mm, and olivine microphenocrysts and subordinate zeolites set in a fine-grained groundmass of cryptocrystalline olivine, plagioclase, clinopyroxene, opaques and interstitial glass.

GGU 362149 70.36944°N, 53.2956°W, 710 m elevation

A pillow breccia sample from the main hyaloclastite breccia wall facing the Vaigat strait, 1 km W of Nuuk Qiterleq. The sample is from the middle part of the Naujánguit Member, taken from the upper part of a 400 m high, foreset-bedded hyaloclastite breccia unit. The near-vertical breccia wall is very actively eroding, and accessible to high levels only via an alluvial fan from an erosion gully. The area is undergoing strong erosion, suggesting a short surface exposure time.

Olivine composition - Fo86.3-92.5. Abundant euhedral to subhedral olivine phenocrysts and glomerocrysts up to ~6 mm, some with corroded, serpentinized and partially replaced cores, and containing spinel and glassy inclusions, along with olivine microphenocrysts and laths of

plagioclase up to 0.5 mm long, set in a fine-grained hyalopilitic groundmass of plagioclase microlites, cryptocrystalline olivine, clinopyroxene, glass and opaques.

GGU 362275 70.41500°N, 53.87583°W, 793 m elevation

A lava sample from mountain side facing the Vaigat strait, 1 km west of the peak Nuusap Qaqqarsuaq (1240 m). The mountain side consists of subaerial lava flows, interspersed with thin breccia horizons above a 400 m high, vertical main breccia wall. The sample is from the lower part of the Naujánguit Member, taken from 1 m above the base of an 11 m thick olivine-rich, massive lava flow. Although there has been significant recent erosion in the area, it was not ice covered during the last glaciation, and may have been exposed for several thousand years.

Olivine composition - Fo86.0-92.5. Abundant subhedral olivine phenocrysts up to 4 mm long containing spinel inclusions and showing signs of post-emplacement cataclasis, and minor amounts of a coarse-grained matrix consisting of ophitic clinopyroxene, small plagioclase laths up to 0.8 mm long, microphenocrysts of olivine, opaques and minor zeolites.

GGU 400457 70.51837°N, 54.1720°W, 100 m elevation

A lava sample from the middle part of the Anaanaa Member. The area is gently sloping low country generally covered by moraine, 2 km due east of Marraat Killiit at the west coast of Nuussuaq. The sample was taken from a 3 m thick lava flow in a series of thin flows, from a well-exposed streambed with modest erosion. The area was covered by thick ice during the last glaciation, suggesting a maximum exposure time of 6000 years.

Olivine composition - Fo86.0-87.2. Euhedral olivine phenocrysts showing strain lamellae and subhedral olivine phenocrysts up to 4 mm long containing spinel inclusions, set in a fine-grained groundmass containing plagioclase microlites up to 0.6 mm, microphenocrysts of olivine and opaques, and interstitial clinopyroxene, zeolites and glass.